# Deeply Virtual Compton Scattering off Nuclei

Eric Voutier

Laboratoire de Physique Subatomique et de Cosmologie
IN2P3/CNRS – Université Joseph Fourier – INP
53 rue des Martyrs
38026 Grenoble cedex, France

**Abstract.** Deeply virtual Compton scattering (DVCS) is the golden exclusive channel for the study of the partonic structure of hadrons, within the universal framework of generalized parton distributions (GPDs). This paper presents the aim and general ideas of the DVCS experimental program off nuclei at the Jefferson Laboratory. The benefits of the study of the coherent and the incoherent channels to the understanding of the EMC (European Muon Collaboration) effect are discussed, along with the case of nuclear targets to access neutron GPDs.

## 1 Introduction

The perspective of an access to the partonic structure of hadrons in the scaling regime of exclusive processes, particularly the contribution of the quark orbital momentum to the nucleon spin [1], sustains an important theoretical and experimental activity. Pioneer measurements at HERMES [2] and CLAS [3] have demonstrated the relevance of the deeply virtual Compton scattering (DVCS) process to these studies. Together with recent dedicated DVCS experiments [4, 5] at the Jefferson Laboratory (JLab) supporting the scaling of the cross section at transferred momentum as low as 2 GeV$^2$, the road towards a systematic investigation of novel features of the inner structure of hadrons is opened.

Generalized Parton Distributions (GPDs) [6, 7] provide a powerful and appealing framework for the description of the partonic structure of hadrons. GPDs represent the interference between amplitudes corresponding to different quantum states and describe the correlations between quarks, anti-quarks, and gluons. They can be interpreted as the transverse distribution of partons carrying a certain longitudinal momentum fraction of the hadron [8–11], providing then a natural link with the transverse degrees of freedom. Therefore, GPDs unify in the same framework electromagnetic form factors, parton distributions, and the spin of the nucleon [12].

The observation by the European Muon Collaboration (EMC) of a deviation of the deep inelastic structure function of a nucleus from the sum of the structure functions of the free nucleons [13] (EMC effect), shows that the nuclear environment has a significant impact on the partonic structure of nucleons. Many years of theoretical and experimental efforts have led to the identification of four different kinematical regimes, however without providing a clear physical interpretation of this phenomenon. GPDs bring a new and specific light on the understanding of the

EMC effect by allowing the investigation of the role of parton correlations as well as the parton distributions of bound nucleons, via the deeply virtual Compton scattering (DVCS) process.

## 2 Principle of Experiments

GPDs are universal non-perturbative objects entering the description of hard scattering processes. They are defined for each quark flavor $f$ and gluon, and correspond to the amplitude for removing a parton of longitudinal momentum fraction $x+\xi$ and restoring it with momentum fraction $x-\xi$ (Figure 1). In this process, the nucleus receives a momentum transfer $t=\Delta^2$ which transverse component $\Delta_\perp$ is Fourier conjugate to the transverse position of partons.

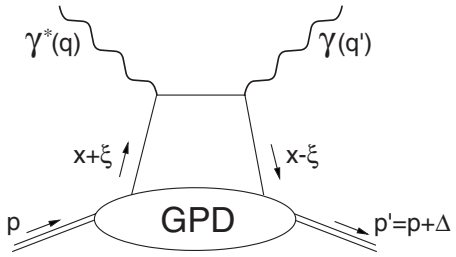


Figure 1. Lowest order (QCD) amplitude for the virtual Compton process. The momentum four-vectors of the incident and scattered photon are $q$ and $q'$, respectively. The momentum four-vectors of the initial and final proton are $p$ and $p'$, with $\Delta$=$(p'-p)$=$(q-q')$. The DIS (deep inelastic scattering) scaling variable is $x_{\rm B}$=$Q^2/(2p\cdot q)$ and the DVCS scaling variable is $\xi$=$x_{\rm B}/(2-x_{\rm B})$. In light cone coordinates defined by $P$=$(p+p')/2$, the initial and final momentum of the photons are $-2\xi$ and 0, respectively.

DVCS, corresponding to the absorption of a virtual photon by a quark followed quasi-instantaneously by the emission of a real photon, is the simplest reaction to access GPDs. In the Bjorken regim, $-t \ll Q^2$ and $Q^2$ much larger than the quark confinement scale, the leading contribution to the reaction amplitude is represented by the so-called handbag diagram (Figure 1) which figures the convolution of a known $\gamma^* q \rightarrow \gamma q$ hard scattering kernel with an unknown soft matrix element describing the partonic structure of the nucleus parametrized by GPDs [14, 15]. Consequently, GPDs ($H^f$) enter the reaction cross section through the Compton form factor $\mathcal{H}$ which involves an integral over the intermediate quark propagators

$$\mathcal{H} = \sum_f e_f^2 \, \mathcal{P} \int_{-1}^{+1} dx \left( \frac{1}{x-\xi} + \frac{1}{x+\xi} \right) H^f(Q^2,x,\xi,t) \qquad (1)$$
$$-i\pi \sum_f e_f^2 \left[ H^f(Q^2,\xi,\xi,t) - H^f(Q^2,-\xi,\xi,t) \right]$$

$e_f$ being the electric charge of the considered quark flavor in unit of the elementary charge.

In addition to the DVCS amplitude, the cross section for electroproduction of photons gets contributions from the Bethe-Heitler (BH) process where the real photon is emitted by the initial or final lepton, leading to

$$\frac{d^5\sigma}{dQ^2 dx_B dt d\phi_e d\varphi} = \mathcal{T}_{BH}^2 + |\mathcal{T}_{DVCS}|^2 + 2\,\mathcal{T}_{BH}\Re e\{\mathcal{T}_{DVCS}\} \tag{2}$$

where $\phi_e$ is the scattered electron azimuthal angle and $\varphi$ is the out-of-plane angle between the leptonic and hadronic planes. The BH and DVCS processes are undistinguishable but the BH amplitude is completely known and exactly calculable from the electromagnetic form factors. Beam and/or target polarization degrees of freedom can be used to select different contributions to the cross section. Particularly, the polarized cross section difference for opposite beam helicities can be used to isolate the imaginary part of the DVCS amplitude, according to the expression [16]

$$\begin{aligned}\frac{d^5\,\Delta\sigma}{dQ^2 dx_B dt d\phi_e d\varphi} &= \frac{1}{2}\left[\frac{d^5\overrightarrow{\sigma}}{dQ^2 dx_B dt d\phi_e d\varphi} - \frac{d^5\overleftarrow{\sigma}}{dQ^2 dx_B dt d\phi_e d\varphi}\right] \\ &= \mathcal{T}_{BH}\,\Im m\{\mathcal{T}_{DVCS}\} + \Re e\{\mathcal{T}_{DVCS}\}\,\Im m\{\mathcal{T}_{DVCS}\}\end{aligned} \tag{3}$$

where $\Im m\{\mathcal{T}_{DVCS}\}$ appears now linearly, instead of quadratically, and magnified by the BH amplitude.

## 3 Nuclear Generalized Parton Distributions

GPDs may be classified according to their helicity and chirality properties [17, 18]. For a spin $S$ nucleus, one can define $(2S+1)\cdot(2S+1)$ parton helicity conserving and chiral even quark GPDs, and $(2S+1)\cdot(2S+1)$ parton helicity flipping and chiral odd quark GPDs. The same number of GPDs is needed for gluons, such that the complete partonic structure of the nucleus may be described by $4\cdot(2S+1)^2$ parton GPDs, half of them conserving the nucleus helicity. DVCS is sensitive only to chiral even GPDs and is dominated by quark or gluon GPDs depending mainly on the studied $x_B$ region.

Similarly to nucleon GPDs, the optical theorem and the polynomiality constraints have remarkable consequences on nuclear GPDs [19, 20]. Considering for example a scalar nucleus target $A$, the quark and gluon GPDs are linked to the forward parton distributions following

$$H^{f/A}(Q^2, x, \xi=0, t=0) = q^{f/A}(Q^2, x) \tag{4}$$

$$H_T^{f/A}(Q^2, x, \xi=0, t=0) = \delta q^{f/A}(Q^2, x) \tag{5}$$

$$H^{g/A}(Q^2, x, \xi=0, t=0) = x g^{A}(Q^2, x) \tag{6}$$

where $q^{f/A}(Q^2,x)$, $\delta q^{f/A}(Q^2,x)$, and $g^A(Q^2,x)$ are the quark flavor $f$ density, transversity, and gluon distributions of the $A$ nucleus, respectively. The gluon

heliciy-flip GPD is zero in the forward limit case. The first Mellin moment relates the quark GPDs to the nucleus electromagnetic form factor

$$\sum_f e_f \int_{-1}^{1} dx\, H^{f/A}(Q^2, x, \xi, t) = F^A(t). \tag{7}$$

A similar relation can be written for the quark chiral odd GPD

$$\sum_f e_f \int_{-1}^{1} dx\, H_T^{f/A}(Q^2, x, \xi, t) = \kappa_T^A(t) \tag{8}$$

where $\kappa_T^A(t)$ represents the spin-flavour dipole moment [21] of the isoscalar nucleus which may be accessed in electroproduction of neutral pions [22]. The second Mellin moment for quark and gluon GPDs writes

$$\int_{-1}^{1} dx\, x H^{f/A}(Q^2, x, \xi, t) = M_2^{f/A}(t) + \frac{4}{5}\xi^2 d^{f/A}(t) \tag{9}$$

where the first term of the right-hand side represents the momentum fraction of the target carried by the quark, and the second term is the nuclear D-term encoding information about the forces experienced by partons inside hadrons [23]. In the particular case of a spin 1/2 nucleus, the D-term dependence drops out in the sum of second Mellin moments of unpolarized chiral even GPDs. Its forward limit yields

$$\frac{1}{2}\int_{-1}^{1} dx\, x\big[H^f(Q^2, x, \xi, 0) + E^f(Q^2, x, \xi, 0)\big] = J^f = \frac{1}{2}\Delta\Sigma^f + L^f, \tag{10}$$

the so-called Ji sum rule [1] which allows access to the contribution of the orbital momentum of partons to the spin of the nucleon.
The previous relation (Eq. (10)) involves the $E^f$ GPD, a completely new distribution flipping the spin of the nucleus and therefore inaccessible to inclusive DIS experiments. Higher spin nuclei figure also several other unknown distributions related to peculiar features of the partonic structure of the nuclei [19].

## 4 Coherent Deeply Virtual Compton Scattering

Coherent DVCS corresponds to the channel of the DVCS reaction off nuclei where the final state consists exclusively of the initial nucleus (Figure 2). This process probes directly the nuclear GPDs i.e. the GPDs of the nucleus, that may be reconstructed from the elementary nucleon GPDs [20, 24–26] depending on specific models of the nuclear structure. As a consequence of the $t$-dependence of the nuclear electromagnetic form factors, the coherent DVCS cross section is strongly suppressed as the momentum transfer to the nucleus increases. This expected behaviour was experimentally observed on several nuclei at HERMES [27] and on the

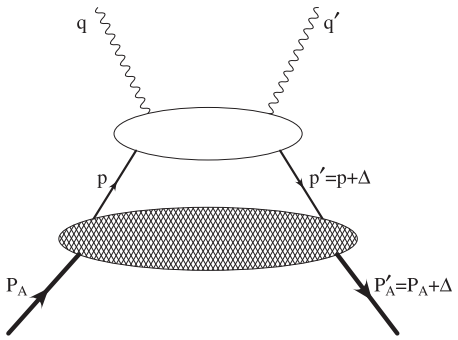


Figure 2. Schematic diagram of the coherent DVCS reaction amplitude: the DVCS process occurs on a quark belonging to a nucleon embedded in the nuclear medium represented by a non-diagonal spectral function $S_F(p, p')$ [25].

deuterium at JLab [28]. More dedicated exclusive experiments are required to obtain quantitative and conclusive information about nuclear GPDs. Particularly, the exclusivity constraint at small $t$ calls for the detection of the recoil nucleus. This is the strategy chosen by an exploratory experiment on the $^4$He which aims to obtain the first quantitative measurements of the imaginary and real parts of the $^4$He Compton form factor [29].

### 4.1 Elementary Case

The $^4$He nucleus may be considered in many respects as an elementary system for the study of the impact of the nuclear medium on the partonic structure of nuclei: it is a well-known few-body system for which the most sophisticated microscopic calculations of the nuclear structure and dynamics are well-established [30]; it is a dense enough nucleus to generate sensitive effects on the parton distributions [31]; in the context of the DVCS process, its leading twist partonic structure is described by one single Compton form factor $\mathcal{H}^A$ (Section 3).

The ratio of the beam polarized cross section difference (Eq. (3)) and unpolarized cross section (Eq. (2)) defines the beam spin asymmetry (BSA) measured for two opposite beam longitudinal helicities. For a spin zero nucleus, the BSA at the twist-2 accuracy writes

$$A_{LU}(\varphi) = \frac{\alpha_0(\varphi)\Im^A}{\alpha_1(\varphi) + \alpha_2(\varphi)\Re^A + \alpha_3(\varphi)(\Re^A \cdot \Re^A + \Im^A \cdot \Im^A)} \tag{11}$$

where $\Im^A = \Im m\{\mathcal{H}^A\}$, $\Re^A = \Re e\{\mathcal{H}^A\}$ are the unknown imaginary and real parts of the Compton form factor, and the $\alpha_i(\varphi)$'s are kinematical factors depending on $\varphi$. Therefore, measuring the $\varphi$ distribution of the BSA at a given kinematics $(Q^2, x_B, t)$ allows to extract simultaneously $\Im^A$ and $\Re^A$ [32]. The simple BSA expression of Eq. (11) is a direct consequence of the spin zero of the $^4$He nucleus.

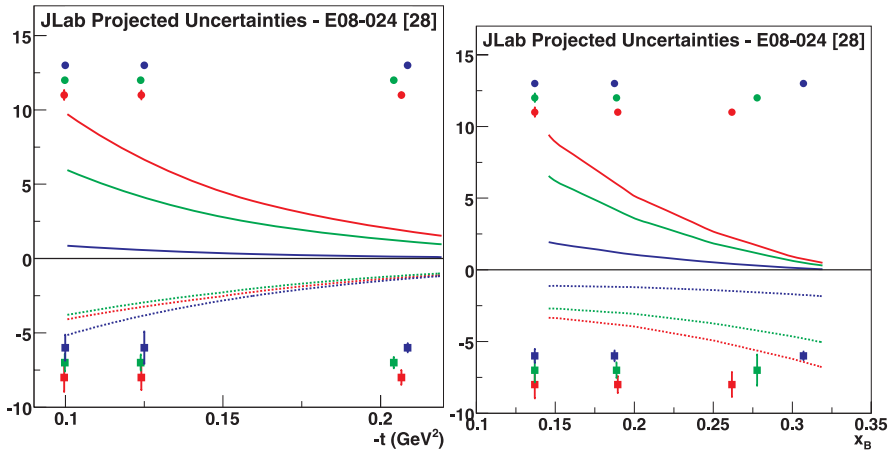


Figure 3. Comparison of the projected uncertainties of the E08-024 DVCS experiment off $^4$He [29] at different kinematics, to model predictions [24]; the upper positive part of each panel represents $\Im^A$ predictions, and the lower negative part, $\Re^A$'s; the blue, red, and green colors on the left panel correspond to $x_B = 0.13,\ 0.19,\ 0.28$, and on the right panel to $-t = 0.09,\ 0.12,\ 0.20$ GeV$^2$, respectively.

Higher spin targets figure a combination of Compton form factors that does not factorize in a simple bilinear form [33]. More strictly, gauge invariance of the DVCS amplitude [34] complicates this simple expression by introducing twist-3 GPDs in the numerator and denominator of Eq. (11) [35]. Twist-3 nuclear GPDs are mostly unknown distributions, and in the case of the $^4$He nucleus, one may expect to get some information from the BSA in the region of the minimum of the electromagnetic form factor, i.e. in a region where the BSA depends only on pure DVCS quantities.

Relying on this experimental technique, the E08-024 experiment at JLab [29] will provide high quality data to control the importance of the twist-3 contributions and extract the twist-2 $^4$He Compton form factor in the valence region (Figure 3). The exclusivity of the reaction channel will be ensured by the detection of the scattered electrons with CLAS [36], the produced real photons with a specific internal calorimeter at small angles ($4^\circ \leq \theta_\gamma^{lab.} \leq 15^\circ$) supplementing CLAS capabilities at larger angles, and the recoil nuclei with the BoNuS radial time-projection chamber [37]. The $Q^2$, $x_B$, and $-t$ dependencies of $\mathcal{H}^A$ will be measured, however in a limited phase space. An exhaustive investigation of coherent DVCS requires the full capabilities of the 12 GeV upgrade. The present experiment should provide a guide for these future studies of the femto-tomography of the nucleus.

### 4.2 Generalized EMC Ratio

Nuclear effects are often expressed as the ratio of a given observable on a nuclear target with the same observable measured on an hydrogen target. The ratio $R_A$ of

the amplitude of the nuclear and nucleon BSAs is then expected to be an indication of the nuclear medium effects on the partonic structure of the nucleus. In the case of an isoscalar target, and assuming the dominance of the BH cross section, this ratio may be written

$$R_A(Q^2, x_B, t) = \frac{A_{LU}^{^4He}(Q^2, x_B, t, \varphi = \frac{\pi}{2})}{A_{LU}^{^1H}(Q^2, x_B, t, \varphi = \frac{\pi}{2})} \tag{12}$$

$$\propto \frac{\Im m\left\{F^A \mathcal{H}^A\right\}}{\Im m\left\{F_1\mathcal{H} + \xi(F_1+F_2)\widetilde{\mathcal{H}} - \frac{t}{4M^2}F_2\mathcal{E}\right\}} \frac{\left|\tau_{BH}^{^1H}\right|^2}{\left|\tau_{BH}^{^4He}\right|^2} \tag{13}$$

$$\approx \frac{H^A}{H}\frac{F_1}{F^A} \tag{14}$$

where $F_{1(2)}$ is the Dirac(Pauli) nucleon electromagnetic form factor, and $\{\mathcal{H}, \widetilde{\mathcal{H}}, \mathcal{E}\}$ are the nucleon Compton form factors. The approximated expression of Eq. (14) [38] makes clear the physical meaning of $R_A$, especially in the forward limit where the GPDs reduce to the usual parton distributions: $R_A$ can be interpreted as a generalized (or off-forward) EMC ratio, characterizing nuclear medium effects in the direction transverse to $\vec{q}$. The benefit of this ratio, supported by several calulations [26, 38, 39], is shown in Figure 4. The generalized EMC ratio appears to be a very sensitive observable to the ingredients of the calculations i.e. the measurement of this observable should help to disentangle unambiguously between the many scenarios proposed for the explanation of the EMC effect. In this calculation,

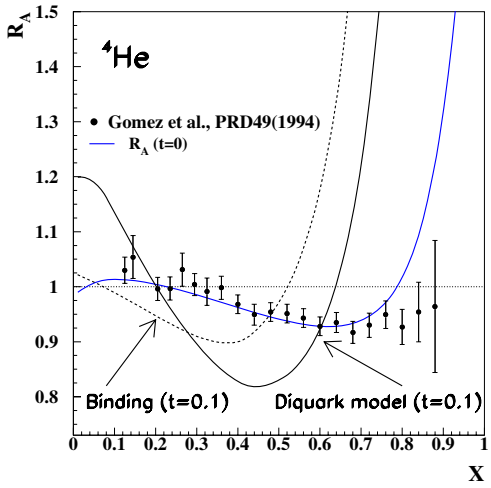


Figure 4. Off-forward EMC effect in $^4$He at $-t = 0.1$ GeV$^2$ [38]; theoretical calculations are shown for two different descriptions of the EMC effect, and are compared with experimental data [40] and predictions for the forward case.

the striking stronger effects in the off-forward case suggest that the correlations between partons may play a crucial role in this problem.

## 5 Incoherent Deeply Virtual Compton Scattering

Incoherent DVCS is a complementary chanel to coherent DVCS where, in addition to the production of a real photon, a nucleon is expelled from the intial nucleus. In the impulse approximation, this process may be described as the interaction of the virtual photon with a quark belonging to a nucleon embedded in the nuclear medium (Figure 5). The elementary GPD information is basically the same for coherent and incoherent DVCS, the essential difference arising from the nuclear information: incoherent DVCS involves the usual nuclear spectral function $S(p,E)$ while coherent DVCS considers a generalized skewed spectral function $S_F(p,p')$ [25, 39]. Consequently, incoherent DVCS can be considered as a direct way to access bound nucleon GPDs which quantify the effect of the nuclear medium on free nucleon GPDs [38, 41].

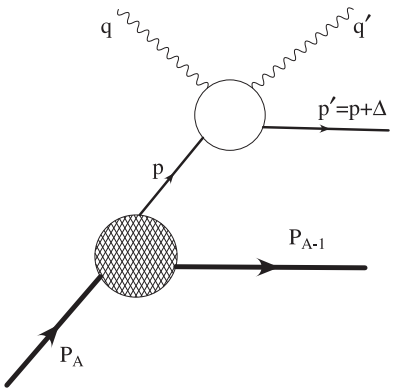


Figure 5. Schematic representation of the incoherent DVCS process in the impulse approximation: the elementary DVCS process is convoluted with the probability to find a nucleon with momentum $p$ and energy $E$ in the initial nucleus i.e. the nuclear spectral function $S(p,E)$.

### 5.1 Laboratory for Bound Nucleons

The A$(e,e'p\gamma)$A-1 reaction isolates specifically partonic configurations of bound nucleons, and opens a new path for the investigation of bound nucleon properties. Here, the perpendicular component of the momentum transfer to the nucleon is the Fourier conjugate to the transverse position of partons inside the bound nucleon, an information required to access features like the confinement size of bound nucleons

or the transverse overlap areas of hadronic configurations in the nucleus. Similarly to the coherent case, nuclear medium effects may be expressed in terms of the BSA ratio $R_{p/A}$ for the incoherent and free nucleon processes

$$R_{p/A}(Q^2, x_B, t) = \frac{A_{LU}^{p/A}(Q^2, x_B, t, \varphi = \frac{\pi}{2})}{A_{LU}^{^1H}(Q^2, x_B, t, \varphi = \frac{\pi}{2})} \tag{15}$$

$$\propto \frac{\Im m\left\{F_1^{p/A}\mathcal{H}^{p/A} + \xi(F_1^{p/A} + F_2^{p/A})\widetilde{\mathcal{H}}^{p/A} - \frac{t}{4M^2}F_2^{p/A}\mathcal{E}^{p/A}\right\}}{\Im m\left\{F_1\mathcal{H} + \xi(F_1 + F_2)\widetilde{\mathcal{H}} - \frac{t}{4M^2}F_2\mathcal{E}\right\}} \frac{\left|\tau_{BH}^{^1H}\right|^2}{\left|\tau_{BH}^{p/A}\right|^2} \tag{16}$$

where $F_{1(2)}^{p/A}$ is the Dirac(Pauli) bound nucleon electromagnetic form factor, and $\{\mathcal{H}^{p/A}, \widetilde{\mathcal{H}}^{p/A}, \mathcal{E}^{p/A}\}$ are the bound nucleon Compton form factors. $R_{p/A}$ turns out to be a very sensitive observable to the details of the medium modification models [25, 39]. Future measurements of this observable off the $^4$He nucleus [29] are strongly expected to help our understanding of bound nucleon properties.

However, as in the A$(e, e'p)$A-1 reaction, one should be attentive to the effects of the initial Fermi motion and to the reaction mechanisms beyond impulse approximation. This is of particular importance for the BH process which is used as a reference light to reveal deviations originating from the DVCS mechanism. In this respect, the conservation of the electromagnetic current together with a reliable description of off-shellness effects are mandatory. Final state interactions between the recoil nucleon and the residual nucleus are also expected to impact the extraction of the DVCS signal from the distortion of the simple scheme of the impulse approximation via interferring amplitudes and imaginary BH. The magnitude of these several effects are currently investigated [42].

### 5.2 Effective Neutron Target

In abscence of free neutron targets, few-body systems are often used as effective neutron targets. Typically, the deuterium is considered as a free neutron target and polarized $^3$He as an effective polarized neutron target; higher mass nuclei feature important contributions from other reaction mechanisms which make the spectator nucleon picture unreliable [43].

DVCS off the neutron appears as a process complementary to DVCS off the proton, and is a mandatory step in the hunt for the quark angular momentum [28]. Indeed, the differences between neutron and proton electromagnetic form factors allow to access new combinations of GPDs. Furthermore, because of the electric charge weighting each flavor GPD (Eq. (1)), the neutron is essentially sensitive to the $u$ quark flavor, similarly to the proton. Consequently to isospin symmetry, the measurement of neutron GPDs tells about the $d$ quark GPDs in the proton. This is exactly the message that was delivered by the JLab Hall A n-DVCS experiment [51]. The complementary between neutron and proton data was expressed in terms of a model dependent extraction of the $u$ and $d$ quark angular momenta (Figure 6) which

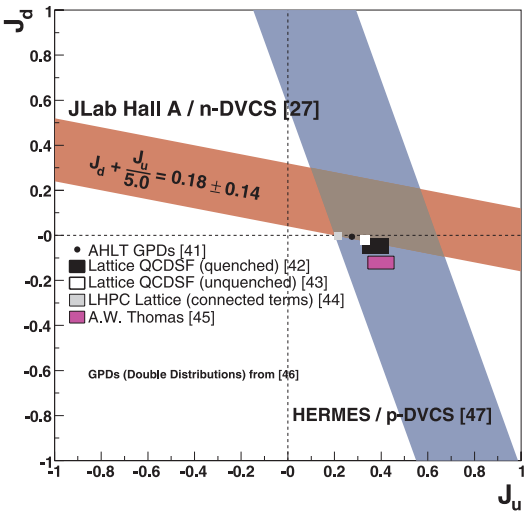


Figure 6. Model dependent experimental constraint on $J_u$ and $J_d$ quark angular momenta from the JLab Hall A n-DVCS experiment [28]. Different model calculations [44–48] are compared to an extrapolation of experimental data within the VGG double distribution description of GPDs [49]. A similar constraint from the $\vec{\text{p}}$-DVCS target spin asymmetry measured by HERMES [50] is also shown.

shows that the beam polarized cross section difference off the neutron is, similarly to the transversely polarized target spin asymmetry, sensitive to the least known and constrained GPD $E$ [28] of particular importance in the angular momentum sum rule [1].

This last feature can be clearly understood from the inspection of the single polarization DVCS observables for the neutron. In the small $t$ limit, the neutron Dirac form factor vanishes, as does the spin conserving polarized GPD $\widetilde{H}$ as a result of the cancelation between the $\Delta u$ and $\Delta d$ quark helicity distributions. Within this approximation and at the twist-2 accuracy, the GPD dependent part [33] of the cross section difference for a longitudinally polarized beam and an unpolarized target may be expressed

$$\frac{d^5\overrightarrow{\sigma}}{d^5\Omega} - \frac{d^5\overleftarrow{\sigma}}{d^5\Omega} \propto -\frac{t}{4M^2}\, F_2\, \Im m\left[\mathcal{E}\right]\, \sin(\varphi) \tag{17}$$

where $d^5\Omega \equiv dQ^2 dx_B dt d\phi_e d\varphi$. Similarly, the GPD dependent part [33] of the cross section difference for an unpolarized beam and a longitudinally polarized target may be written

$$\frac{d^5\sigma^{\rightarrow}}{d^5\Omega} - \frac{d^5\sigma^{\leftarrow}}{d^5\Omega} \propto \xi\, F_2\, \Im m\left[\mathcal{H} + \frac{\xi}{1+\xi}\mathcal{E} - \frac{t}{4M^2}\widetilde{\mathcal{E}}\right]\, \sin(\varphi)\,, \tag{18}$$

and for a transversely polarized target with azimutal angle $\phi_S$

$$\frac{d^5\sigma^{\uparrow}}{d^5\Omega} - \frac{d^5\sigma^{\downarrow}}{d^5\Omega} \propto \left[c_0^{DVCS} + c_0^I\right]\sin(\varphi-\phi_S) + c_1^I\sin(\varphi-\phi_S)\cos(\varphi) + s_1^I\cos(\varphi-\phi_S)\sin(\varphi) \tag{19}$$

where the coefficients of the harmonic development writes

$$c_0^{DVCS} \propto (1+\xi)\,\Im m\left[\mathcal{H}\mathcal{E}^{\star} - \mathcal{E}\mathcal{H}^{\star}\right] \tag{20}$$

$$c_0^I \propto \frac{1}{1+\xi}\frac{t}{2M^2}\frac{(2-y)^2}{1-y}F_2\,\Im m\left[\xi^2\left(\mathcal{E}-\widetilde{\mathcal{E}}\right) - \left(1-\xi^2\right)\mathcal{H}\right] + \frac{t}{M^2}F_2\,\Im m\left[\mathcal{H}\right] \tag{21}$$

$$c_1^I \propto \frac{1}{1+\xi}\frac{t}{2M^2}F_2\,\Im m\left[\xi^2\left(\mathcal{E}-\widetilde{\mathcal{E}}\right) - \left(1-\xi^2\right)\mathcal{H}\right] \tag{22}$$

$$s_1^I \propto \frac{2\xi}{1+\xi}F_2\,\Im m\left[\xi\mathcal{H} + \frac{\xi^2}{1+\xi}\mathcal{E} + \frac{t}{4M^2}\left(\mathcal{E}-\xi\widetilde{\mathcal{E}}\right)\right]. \tag{23}$$

In the JLab energy range $\xi$ remains smaller than 0.5, such that the dominant contribution in Eq. (18), Eq. (21), Eq. (22), and Eq. (23) is proportional to $\mathcal{H}$. For the transversely polarized target the sensitivity to $E$ appears through a pure DVCS harmonic coefficient, while the most efficient single spin observable to access $E$ seems to be the polarized beam cross section difference.

## 6 Conclusions

DVCS off nuclei is a very promising tool for the investigation of the partonic structure of nuclei. Preliminar measurements at HERMES and JLab have established the existence of a DVCS signal in beam spin asymmetries, but remain quantitatively limited. A full dedicated program starts to develop in the context of the JLab upgrade at 12 GeV, and will benefit from the exploratory experiments on the $^2$H [52] and $^4$He nuclei. Exclusivity is a key feature for the completion of this program.
As today, the incoherent DVCS process is the main source of information for DVCS off the neutron. The perspective to use this channel to investigate the partonic structure of bound nucleons is motivating a lot of theoretical interest, but requires the next generation of experiments for quantitative and conclusive information. The limits of the impulse approximation remains a matter of concern.

## Acknowledgments

I would like to thank the organizers of the XXVIIth International Workshop on Nuclear Theory for their invitation and warm hospitality at Rila Mountains. The development of a nuclear DVCS program at JLab is a collaborative work which benefits from many contributions. I would like to thank H. Egiyan, F.-X. Girod,

V. Guzey, K. Hafidi, C. Hyde, S. Liuti, M. Mazouz and B. Pire for many stimulating and fruitfull discussions.

This work was supported in part by the U.S. Department of Energy (DOE) contract DOE-AC05-06OR23177 under which the Jefferson Science Associates, LLC, operates the Thomas Jefferson National Accelerator Facility, the National Science Foundation, the French Atomic Energy Commission and National Center of Scientific Research, and the GDR n°3034 Physique du Nucléon.

## References

1. X. Ji, Phys. Rev. Lett. **78**, 610 (1997).
2. A. Airapetian *et al.*, Phys. Rev. Lett. **87**, 182001 (2001).
3. S. Stepanyan *et al.*, Phys. Rev. Lett. **87**, 182002 (2001).
4. C. Muñoz Camacho, A. Camsonne, M. Mazouz, C. Ferdi, G. Gavalian, E. Kuchina *et al.*, Phys. Rev. Lett. **97**, 262002 (2006).
5. F.-X. Girod, R.A. Niyazov *et al.*, Phys. Rev. Lett. **100**, 162002 (2008).
6. D. Müller, D. Robaschick, B. Geyer, F.M. Dittes, J. Hořejši, Fortschr. Phys. **42**, 101 (1994).
7. A.V. Radyushkin, Phys. Rev. **D 56**, 5524 (1997).
8. M. Burkardt, Phys. Rev. **D 62**, 071503(R) (2000).
9. J.P. Ralston, B. Pire, Phys. Rev. **D 66**, 111501(R) (2002).
10. M. Diehl, Eur. Phys. Jour. **C 25**, 223 (2002).
11. A.V. Belitsky, D. Müller, Nucl. Phys. **A 711**, 118c (2002).
12. M. Diehl, Phys. Rep. **388**, 41 (2003).
13. J.J. Aubert *et al.*, Phys. Lett. **B 123**, 275 (1983).
14. X. Ji, J. Osborne, Phys. Rev. **D 58**, 094018 (1998).
15. J.C. Collins, A. Freund, Phys. Rev. **D 59**, 074009 (1999).
16. P.A.M. Guichon, M. Vanderhaeghen, Prog. Part. Nucl. Phys. **41**, 125 (1998).
17. M. Diehl, Eur. Phys. J. **C 19**, 485 (2001).
18. S. Boffi, B. Pasquini, Riv. Nuo. Cim. **30**, 387 (2007).
19. E.R. Berger, F. Cano, M. Diehl, B. Pire Phys. Rev. Lett. **87**, 142302 (2001).
20. A. Kirchner, D. Müller, Eur. Phys. J. **C 32**, 347 (2004).
21. M. Burkardt, Phys. Rev. **D 72**, 094020 (2005).
22. S. Ahmad, G.R. Goldstein, S. Liuti, ArXiv:hep-ph **0805.3568** (2008).
23. M. Polyakov, Phys. Lett. **B 555**, 57 (2003).
24. V. Guzey, M. Strikman, Phys. Rev. **C 68**, 015204 (2003).
25. S. Liuti, S.K. Taneja, Phys. Rev. **C 72**, 032201(R) (2005).
26. V. Guzey, ArXiv:hep-ph **0801.3235** (2008).
27. F. Ellinghaus, ArXiv:hep-ex **0710.5768** (2007).
28. M. Mazouz, A. Camsonne, C. Muñoz Camacho, C. Ferdi, G. Gavalian, E. Kuchina *et al.*, Phys. Rev. Lett. **99**, 242501 (2007).
29. H. Egiyan, F.-X. Girod, K. Hafidi, S. Liuti, E. Voutier *et al.*, JLab Proposal **E08-024** (2008).
30. J. Carlson, R. Schiavilla, Rev. Mod. Phys. **70**, 743 (1998).
31. D.F. Geesaman, K. Saito, A.W. Thomas, Ann. Rev. Nucl. Part. Sci. **45**, 337 (1995).
32. Y. Perrin, Master Thesis, Université Joseph Fourier, Grenoble (France), 2008.
33. A.V. Belitsky, D. Müller, A. Kirchner, Nucl. Phys. **B 629**, 323 (2002).

34. I.V. Anikin, B. Pire, O.V. Terayev, Phys. Rev. **D 62**, 071501 (2000).
35. A.V. Belitsky, D. Müller, A. Kirchner, A. Schäfer, Phys. Rev. **D 64**, 116002 (2001).
36. B.A. Mecking *et al.*, Nucl. Inst. Meth. **A 503**, 513 (2003).
37. H. Fenker *et al.*, *Nucl. Inst. Meth.* **A 592**, 273 (2008).
38. S. Liuti, S.K. Taneja, Phys. Rev. **C 72**, 034902 (2005).
39. S. Scopetta, *Phys. Rev.* **C 70**, 015205 (2004).
40. J. Gomez *et al.*, Phys. Rev. **D 49**, 4348 (1994).
41. V. Guzey, A.W. Thomas, K. Tsushima, ArXiv:hep-ph **0806.3288** (2008).
42. S. Liuti, E. Voutier, *work in progress*.
43. A. Misiejuk, Z. Papandreou, E. Voutier *et al.*, Phys. Rev. Lett. **89**, 172501 (2002).
44. S. Ahmad, H. Honkanen, S. Liuti, S.K. Taneja, Phys. Rev. **D 75**, 094003 (2007).
45. M. Göckeler *et al.*, Phys. Rev. Lett. **92**, 042002 (2004).
46. G. Schierholz, Proc. of the Workshop on Exclusive Reactions at High Momentum Transfer, Jefferson Laboratory, Newport News (VA, USA), May 21–24, 2007.
47. Ph. Hägler *et al.*, ArXiv:hep-lat **0705.4295** (2008).
48. A.W. Thomas, ArXiv:hep-ph **0803.2775** (2008).
49. M. Vanderhaeghen, P.A.M. Guichon, M. Guidal, Phys. Rev. **D 60**, 094017 (1999).
50. A. Airapetian *et al.*, ArXiv:hep-ex **0802.2499** (2008).
51. P.Y. Bertin, C. Hyde, F. Sabatié, E. Voutier *et al.*, JLab Proposal **E03-106** (2003).
52. A. Camsonne, C. Hyde, M. Mazouz *et al.*, JLab Proposal **E08-025** (2008).